


T. PASSERAT DE SILANS  
B. FARIAS  
M. ORIÁ  
M. CHEVROLLIER 

# Laser-induced quantum adsorption of neutral atoms in dielectric surfaces

Laboratório de Física Atômica e Lasers, Departamento de Física – Universidade Federal da Paraíba, Cx. Postal 5008, 58051-970 João Pessoa – PB – Brazil

Received: 26 July 2005

Published online: 5 November 2005 • © Springer-Verlag 2005

**ABSTRACT** We propose an optical technique to load neutral atoms in quantum adsorption states of a dielectric surface. Considering a realistic atom–surface potential well, we show that free cold lithium atoms approaching a LiF surface may be transferred to a surface bound state of the first excited atomic state. We also discuss schemes to populate adsorption energy levels of the atomic electronic ground state, and we find that spontaneous mechanisms transfer more than 90% of the excited adsorbed atoms into vibrational levels of the fundamental adsorption potential. The lifetime of the resulting two-dimensional waveguide is calculated, considering the adatoms' interaction with the crystal phonons.

**PACS** 34.50.Dy; 68.43.-h; 68.35.Ja; 32.80.Pj

## 1 Introduction

The study of atoms close to solid surfaces has gained renewed interest with the recent progress in cold-atom manipulations such as, for example, atom optics close to surfaces [1] and nanotechnology [2], where the techniques to grow new devices on substrates have come to submicron resolution [3], requiring then a good understanding of the inherent atom–surface interactions. A better knowledge is therefore needed of both the long- and the short-range parts of these interactions, as well as of the surface-induced electric and magnetic perturbations which limit the stability of cold or ultra-cold atomic clouds close to surfaces.

Since the end of the 1970s, light-atom scattering by clean surfaces has been a valuable tool to derive information on the atom–surface potential. Through the analysis of the angular spectrum this technique allows the determination of the surface bound states [4], but with limited precision [5].

More recently, the ability of manipulating neutral atoms in the proximity of surfaces has established cold atoms as a tool for such up-to-date applications as atom chips and quantum computation [6] as well as a probe very sensitive to the surface-induced perturbations [7]. Various potentials near the surface, such as the optical [8] and magnetic ones [9], have

already been considered to trap atoms at distances to the surface of the order of a few microns. The intrinsic atom–surface potential may be explored as a natural 1D trap for atoms (2D matter wave guide). This waveguide is much deeper than the artificial ones [8, 9] mentioned before, meaning higher mode spacing and thus easier monomode operation of the guide. More basically, atoms trapped in a well-defined vibrational level of the atom–surface potential well would give information on the fundamental short- and long-range (particularly the van der Waals  $C_3$  coefficient) interactions between atoms and surfaces [10].


In the present work we theoretically study the photoassociation of cold atoms with a dielectric surface as a way to achieve high-resolution spectroscopy of the surface bound levels as well as to control the loading of a surface trap: bound levels of the surface potential well are selectively populated (selective quantum adsorption) through the interaction of cold atoms with resonant lasers. The resulting 2D gas may be prepared in the excited or in the ground atomic state through spontaneous or stimulated emission (two-color process). In our previous studies [10], we had considered a very shallow ( $10^{-5}$  eV) surface well in order to study only the long-range atom–surface bound levels. Here we make calculations for realistic parameters of the interaction between lithium atoms and a crystalline dielectric surface of lithium fluoride, four orders of magnitude deeper than the potential considered in Ref. [10]. As very precise results for this system depend on a good knowledge of the potential parameters (short-range amplitude, interaction range, van der Waals coefficient) that are not available in the literature, our goal here is to find an insight into the general behavior of this mechanism of laser-induced quantum adsorption in a realistic surface potential, to guide our experimental choice of a practical system.

## 2 Adsorption potential

The interaction potential between a neutral atom and a crystalline surface is periodic along the surface and may thus be expanded in a 2D Fourier series:

$$V(\mathbf{r}) = V_0(z) + \sum_{\mathbf{G} \neq 0} V_{\mathbf{G}}(z) e^{i\mathbf{G} \cdot \mathbf{R}}, \quad (1)$$

where  $\mathbf{r}$  is the position vector of the atom,  $\mathbf{G}$  is a 2D reciprocal lattice vector,  $\mathbf{R} = (x, y)$  is the  $\mathbf{r}$  component parallel to the sur-

 Fax: (55)8332167513, E-mail: martine@otica.ufpb.br

face and  $z$  is the distance along the normal to the surface.  $V_0(z)$  is the surface-averaged potential. The effects of the corrugation on the eigenstates of this 1D laterally averaged potential can be determined by considering the other terms of the expansion (for  $\mathbf{G} \neq 0$ ) as perturbations relative to the ‘main’ term  $V_0$ . This periodic correction plays an essential role in experiments of diffractive scattering of light atoms by crystalline surfaces [4] and of quantum transportation such as Bloch oscillations [11]. However, in this work, we restrict ourselves to the first term of the interaction potential in Eq. (1) [12], because our aim is to find an insight into the quantum kinematics of the atomic center-of-mass to populate the 1D adsorption potential. The atom–surface interaction at long range is the van der Waals attraction, scaling as  $-1/z^3$ . At short range the interaction is due to the Pauli repulsion and can be modeled by an exponentially decaying term [13]. Considering the quite large uncertainty still allowed by the actual state of knowledge of the interactions in these systems, we assume that a good semi-quantitative insight can be obtained through the analytical study of the Morse potential [14]:

$$V_0(z) = A(\exp(-2\alpha z) - 2\exp(-\alpha z)). \quad (2)$$

Further experimental investigation should provide the data necessary to numerically improve the treatment of a more realistic potential. The values of the amplitude and range parameters, respectively  $A$  and  $\alpha$  in Eq. (2), are taken so that the Morse potential and the physical adsorption potential have the same depth and width, deduced from values of the adsorption energy  $E_a$  and of the  $C_3$  coefficient occasionally available in the literature for the Li–LiF system we study here. Such a system has been chosen because: (i) the number of levels of the adsorption potential is lower for light atoms, (ii) alkali atoms are known to be easily manipulated by lasers [15] and (iii) crystalline surfaces have low and regular roughness and very low electrical conductivity [16].

However, due to the lack of quantitative information about the Li–LiF system in the literature, we used semi-empirical rules as in Ref. [19] to adapt available data to our specific problem. These rules are given by

$$C_3 = K\alpha_0 \frac{n^2 - 1}{n^2 + 1} \quad \text{and} \quad (3)$$

$$E_a = \frac{1}{r^3} K\alpha_0 \frac{n^2 - 1}{n^2 + 1}, \quad (4)$$

with  $\alpha_0$  and  $r$  the atomic static polarizability and radius, respectively,  $n$  the refractive index of the transparent dielectric and  $K$  a proportionality constant. The  $(n^2 - 1)/(n^2 + 1)$  term expresses the attenuation of the van der Waals force in comparison with a metallic surface (perfect mirror). The interaction potential parameters for the Li–LiF system are therefore estimated as follows: for the Li electronic ground state ( $2S_{1/2}$ ), we extrapolated the  $C_3$  coefficient for a perfectly conducting wall ( $C_{3,\text{Li}}^{\text{metal}} = 1.52$  a.u.) [17] to a LiF surface ( $n^{\text{LiF}} = 1.4$ ) through Eq. (3). In the same way, we adapted data of the adsorption energy  $E_a$  of the Cs–sapphire system ( $E_{a,\text{Cs}}^{\text{sapphire}} = 0.5$  eV [18],  $n^{\text{sapphire}} = 1.76$ ) to the Li–LiF one, using the semi-empirical rules of Eqs. (3) and (4), with the

radii of the Cs and Li atoms  $r_{\text{Cs}} = 3.33$  Å and  $r_{\text{Li}} = 2.05$  Å [20] and the polarizabilities  $\alpha_{0,\text{Cs}} = 400$  a<sub>0</sub><sup>3</sup> and  $\alpha_{0,\text{Li}} = 164$  a<sub>0</sub><sup>3</sup> [21]. These semi-empirical rules were also used to determine the  $C_3$  and  $E_a$  values for the electronic excited state  $2P_{1/2}$  of the Li–LiF system ( $\alpha_{0,\text{Li}}^* = 130$  a<sub>0</sub><sup>3</sup> [21]). We have thus obtained  $C_{3,\text{Li}}^{\text{LiF}} = 0.5$  a.u. and  $E_{a,\text{Li}}^{\text{LiF}} = 0.60$  eV for the ground state and  $C_{3,\text{Li}^*}^{\text{LiF}} = 0.4$  a.u. and  $E_{a,\text{Li}^*}^{\text{LiF}} = 0.47$  eV for the excited state. The parameters of the Morse potential in Eq. (2) are therefore  $A = E_a$  and  $\alpha = 1.98$  Å<sup>-1</sup> (2.24 Å<sup>-1</sup>) for the ground (excited) electronic state.

### 3 Photoassociation process

We solve the Schrödinger equation for the Morse potential of Eq. (2) and the parameters detailed above. We obtain 23 bound levels in the Li ground electronic state  $2S_{1/2}$  and 18 in the first excited electronic state  $2P_{1/2}$ . The smallest energy spacing between two vibrational levels of an electronic state (between  $v = 21$  and  $v = 22$  of the ground state) is  $\approx 374$  GHz (1.55 meV), corresponding to a temperature of  $\approx 36$  K that is much higher than the temperature of the cold atomic source, a magneto-optical trap (MOT), considered in our calculations. This should allow one to populate and detect even the highest bound levels of the excited state with a very good resolution and ultimately to load atoms into this surface waveguide in a well-defined adsorption level.

The surface well may be loaded with Li atoms from a MOT built very close to a dielectric window [22], and having an energy corresponding to the temperature of 142  $\mu$ K. The scheme to load bound levels of the electronic states is illustrated in Fig. 1. A free atom in a level  $|f\rangle$  with energy  $E$  (and well-defined momentum  $p = \sqrt{2mE} = \hbar k$ , where  $m$  is the mass of the atom and  $k$  is the de Broglie wavenumber) absorbs a laser photon of frequency  $\omega_1$  and goes to a high bound level  $|v'\rangle$  of the first excited electronic state of the atom. This

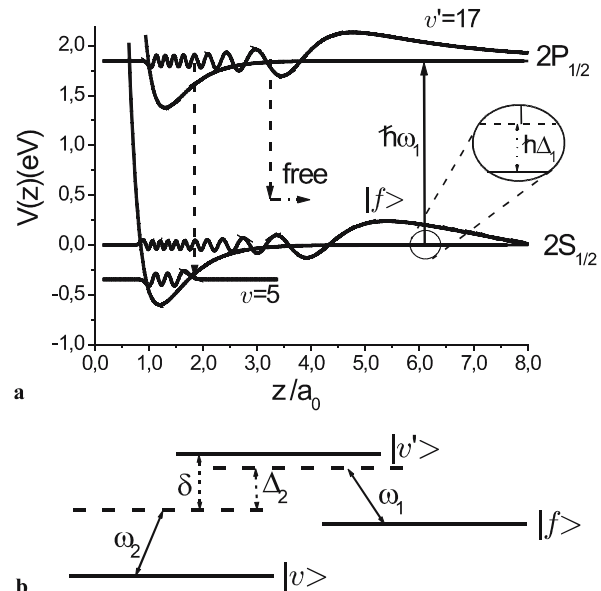
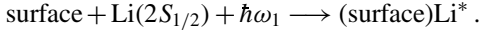


**FIGURE 1** (a) Photoassociation scheme for cold Li atoms and a LiF surface.  $2S_{1/2}$ - and  $2P_{1/2}$ -asymptotic surface potentials are shown, together with the incoming free wave function and vibrational wave functions. (b) Energy levels and detunings involved in the Raman process (see text)

is a photoassociation (PA) process between the surface and the atom:



The absorption is followed by spontaneous decay, either into the continuum or into discrete bound levels  $v$  of the ground state (asymptote  $2S_{1/2}$ ). Alternatively, a second laser may transfer the atoms to specific ground bound levels through a Raman process, thus allowing a selective population of these levels (see Fig. 1b). The efficiency of the overall scheme is determined by the photoassociation rate and by the emission transition probabilities of the excited adatoms.

We treat the free incident level as a level of a quasi-continuum [23]. In this approach, the PA rate to a bound level  $v'$  has the form

$$R(v') = \frac{1}{2} \rho S \lambda_D \Gamma(v') \exp\left(-\frac{\hbar\Delta_1}{k_B T}\right), \quad (5)$$

where  $\hbar\Delta_1$  is the difference between the energy of the laser photons and the energy of the bound level  $v'$  (above the ground state continuum threshold, see detail in Fig. 1a),  $\rho$  is the atomic density, assumed to be constant,  $S$  is the section of the laser beam irradiating the cold-atom sample,  $\Gamma$  is the photodissociation rate, i.e. the stimulated rate at which the excited bound level decays back to the free ground level, and the thermal de Broglie wavelength is  $\lambda_D = (2\pi\hbar^2/\mu k_B T)^{1/2}$ . Using results of Ref. [23] the photodissociation rate is given by  $\Gamma(v') = (d^2(v')\mathcal{E}^2/2\hbar^2 v_0)L$ , where  $L$  is the dimension of the 1D box of normalization of the incident free wavefunction ( $L \gg k^{-1}$ ).  $\mathcal{E}$  is the amplitude of the electric field,  $v_0 = (2\hbar\Delta_1/m)^{1/2}$  the velocity of the atoms in the free level resonant with the PA laser.  $d$  is the dipole matrix element,  $d^2 = d_0^2 q_{fv'}$ , with the Franck–Condon (FC) factors  $q_{fv'} = |\langle v' | f \rangle|^2$

and  $d_0$  the electronic transition moment, assuming its asymptotic value for  $z \rightarrow \infty$ . For the transition  $2S_{1/2} \rightarrow 2P_{1/2}$ ,  $d_0 = 1.987 \times 10^{-29}$  Cm. The amplitude of the normalized free wavefunction scales as  $L^{-1/2}$ , so that the photodissociation rate  $\Gamma$  is independent of  $L$ .

In Fig. 2a we plot the FC factors for transitions from a free level with an asymptotic energy  $E = 6.3$  neV to the highest surface bound levels of the electronic  $2P_{1/2}$  state. As the PA rate is proportional to the FC factor, it shows the same qualitative behavior, so that the maximum PA rate is obtained for the highest bound level  $v' = 17$  and decreases sharply for the other levels. For typical MOT characteristics  $\rho = 10^{16}$  atoms/m<sup>3</sup> and  $S = 3.14 \times 10^{-6}$  m<sup>2</sup> and with a laser intensity  $I_1 = 10^6$  W/m<sup>2</sup>, the maximum PA rate thus has the value  $R(v' = 17) = 2.3 \times 10^8$  s<sup>-1</sup>, leading to a stationary population (under the action of the laser mechanisms of photoassociation and photodissociation)  $n(v' = 17) = 1.3 \times 10^5$  adatoms.

## 4 Loading of the ground bound levels

The excited adatoms are unstable and applications indeed require their decaying into bound levels of the electronic ground state. Spontaneous decay can drive the adatoms either to free levels (thus contributing to the losses) or to bound levels of the ground state. On the other hand, the transfer to ground bound levels can be driven more selectively by a two-laser (Raman) process. The time scale of the process and its efficiency depend on the detunings  $\delta$  and  $\Delta_2$  (see Fig. 1b) and on the intensities of the two lasers.

### 4.1 Spontaneous emission

The atom–surface potentials are relatively advantageous to a spontaneous population of the ground bound levels: because both the ground and the excited atom–surface potentials go with  $z^{-3}$  and have therefore comparable spatial extents (high overlap of the excited and ground vibrational wavefunctions), the ratio of the bound–bound transitions over the bound–free transitions is expected to be relatively high. It has to be, for instance, closer to the case of heteronuclear cold molecule formation ( $z^{-6}$  scaling for both the ground and the excited potentials) than to the case of homonuclear cold molecule photoassociation (ground  $z^{-6}$ , excited  $z^{-3}$ ). The Li atom presents the additional favorable peculiarity that the polarizability is slightly lower for its first excited electronic state  $2P$  than for its ground state [21]. Its interaction with the surface then gives a configuration where not only are the shapes of the excited and of the fundamental surface potentials very similar, but the extent of the excited potential is slightly smaller than the fundamental one. This favors even more large bound–bound FC factors [24]. Figure 2b exhibits these FC factors for transitions between bound levels of the excited and of the ground states. The spontaneous emission is shown to drive more than 90% of the excited photoassociated atoms ( $v' = 15$ – $17$ ) to bound levels of the electronic ground state, although mostly in high bound levels  $v > 14$ , as evidenced in Fig. 2b. Under spontaneous emission, the population of a ground bound level increases slowly, yet monotonically, with time (see Fig. 3), reaching an equilibrium value at very long times, so that the equilibrium population is in

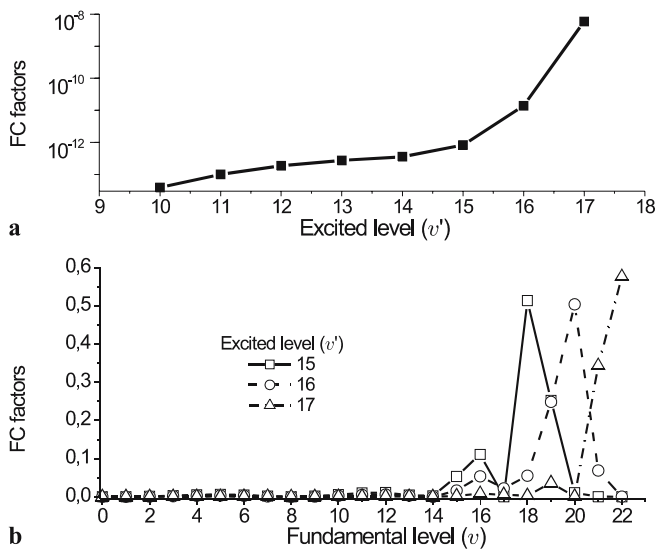


**FIGURE 2** Frank–Condon factors calculated for transitions between surface bound states  $v'$  of the  $2P_{1/2}$ -asymptotic excited electronic level and (a) the free incident state (energy  $E$ ); (b) surface bound states  $v$  of the  $2S_{1/2}$ -asymptotic ground electronic level. In (a) this factor is reduced by more than six orders of magnitude for the deepest levels ( $v' < 11$ )

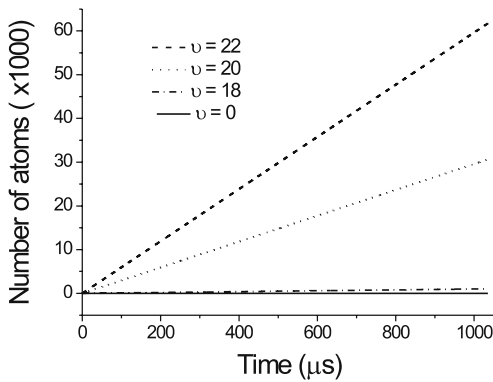


**FIGURE 3** Evolution of the ground bound states' ( $v$ ) population under spontaneous emission from the highest excited bound state  $v' = 17$ , as a function of time

fact a priori limited only by the finite lifetime of the vibrational level (see Sect. 5). The main drawbacks of forming such ground-state adatoms through spontaneous emission from the intermediate levels  $v'$  are that the deepest levels are not directly reached and that the atoms are distributed among a relatively large range of bound levels  $v$  of the electronic ground state, preventing the desired selectivity of the process.

#### 4.2 Stimulated decay

The stimulated formation of ground-state adatoms should overcome the problem of selectivity and enable the population of the deepest ground bound levels. In the case of a two-laser process, the ground bound levels reach an equilibrium population (see Fig. 4, full line and dotted line curves for two different intensities of the second laser). However, the stimulated formation of ground-state adatoms coexists with the reciprocal process of photodissociation, and our calculations of the ground bound levels populations show that, in a continuous-wave configuration, the higher the intensity of the second laser, the lower the equilibrium yields of ground-state adatoms, though the shorter the time to reach this equilibrium (Fig. 4). Moreover, selectivity is not completely achieved, due to spontaneous emission still populating other,

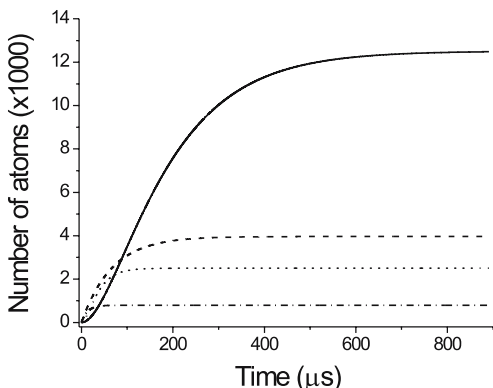


**FIGURE 4** Evolution with time of ground level population, under a two-laser process. Configuration of Fig. 1b, with  $v' = 17$ ,  $\delta = 0$ ,  $\Delta_2 = 0$ ,  $I_1 = 10^6 \text{ W/m}^2$ . Population of  $v = 0$ , full line (dotted line):  $I_2 = 10^4 \text{ W/m}^2$  ( $I_2 = 5 \times 10^4 \text{ W/m}^2$ ); population of  $v = 22$  under spontaneous emission, dashed line (dash-dotted line):  $I_2 = 10^4 \text{ W/m}^2$  ( $I_2 = 5 \times 10^4 \text{ W/m}^2$ )

non-selected, ground bound levels (dashed and dash-dotted curves in Fig. 4).

A pulsed-laser scheme permits both higher yields and better selectivity [23, 25], and a detailed study of this two-laser loading of the surface bound levels will be published elsewhere [26].

In any case, the population of the surface vibrational levels will evolve and, as will be shown below, the interactions with surface phonons should transfer a significant part of the ground-state adatoms to the deepest bound levels, thus balancing the dispersive effect of the spontaneous process.

### 5 Lifetime of the ground bound levels

We estimate the lifetime of the guided atoms in their electronic ground state and in a well-defined vibrational adsorption level. We consider the interaction of the bound atoms with the phonons of the solid, and we neglect two mechanisms of loss: (i) the diffusion toward the solid bulk structure, which is more likely to occur in glass windows [27]; (ii) the heating effects due to electric field fluctuations [28]. Crystalline surfaces with alkali adatoms present very low conductivities in comparison with glass surfaces [16, 29].

We calculated the transition rates between the vibrational levels for an adsorbed atom, considering the atom-phonon coupling in a one-phonon model [30]. With such a coupling the atom can undergo a transition to a free level (desorption) or to a shallower bound level or decay to a deeper bound level (see inset in Fig. 5). The up-transition rates are obviously dependent on the substrate temperature and the allowed transitions are those compatible with the phonon distribution (see results for two surface temperatures in Fig. 5). Rates of desorption are substantial only for the shallowest levels and are zero for the deepest ones, since the energy required for the transition is greater than the Debye energy. A multi-phonon treatment does not qualitatively change this result [30]. We find that, at 10 K, desorption or transitions to shallower levels are much less likely to happen than the decay to deeper levels, resulting in a change of the depletion rate of many orders of magnitude between the deepest levels and those closest to the desorption. The resulting cascade process transfers most of the atomic population to the deepest level of this 2D guide

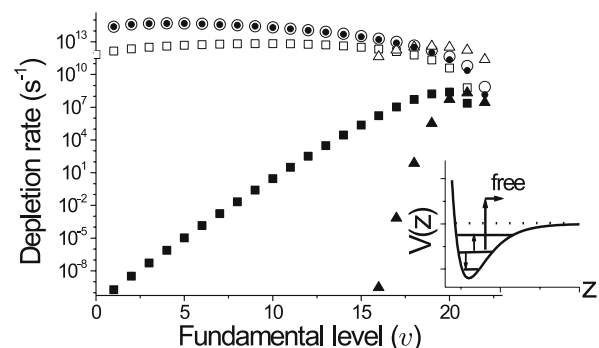


**FIGURE 5** Depletion rate of the surface states for two different temperatures of the substrate: 10 K (solid symbols) and 100 K (hollow symbols). Triangles denote transitions to the continuum; squares: transitions to the level above; circles: transitions to the level below. Inset: one-phonon escape channels for an atom in vibrational levels  $v$  of the adsorption potential

and may be observed at temperatures of the surface easily attainable in laboratories. A simple rate-equation model using these calculated transition rates shows that, at 10 K, the population of the level  $v = 0$  reaches values around  $10^4$  atoms in a time shorter than  $10^{-4}$  s.

## 6 Conclusion

We have proposed an optical technique to load atoms in quantum adsorption levels of a dielectric surface. Calculations of Franck–Condon factors between a free cold level and an excited vibrational level show that it is possible to achieve a great photoassociation rate to the levels closest to dissociation. To load ground levels, the use of a second laser (the first being the PA laser) is shown to substantially increase the population of the deepest bound levels of the electronic ground state, if compared with the spontaneous decay acting alone. The highest yields are obtained for the two-photon resonance  $\delta = \Delta_2 = 0$ , where the intermediate excited level is hardly populated, thus diminishing the amount of atoms spontaneously decaying into the highest bound levels of the electronic ground state. However, this spontaneous process is not suppressed and still leads to a lack of selectivity. A pulsed-laser configuration should severely limit the spontaneous decay, by transferring the atoms into the desired bound levels more rapidly than the spontaneous process. Anyway, at a low surface temperature, energy exchanges with the (low-energy) surface phonons will lead to an accumulation of atoms in the deepest ground bound level in times as short as  $10^{-4}$  s.

Experimental measurements should provide quantitative data for further investigation of this atom–surface system and allow the refinement of the treatment of this laser technique to charge surface quantum levels. A signature of the quantization of the adsorption levels may be obtained by the action of an ionization laser, while scanning the PA laser. The determination of the energy of the highest-lying bound levels should allow the investigation of the van der Waals interaction and particularly to determine the  $C_3$  coefficient [10]. This scheme should be extended to the loading of a Bose–Einstein condensate (BEC) in such surface levels. Further developments of this study include the treatment of the potential periodicity in the planes parallel to the surface, where a band structure of the energy levels is expected [31], and applications such as Bloch oscillations are currently being investigated [11]. One can also expect applications in quantum computation for localized atoms in periodic surface waveguides [32].

**ACKNOWLEDGEMENTS** We acknowledge support from FINEP (FÈNIX project) and CAPES-COFECUB (Project No. 456/04) and partial support from CNPq.

## REFERENCES

- 1 J. Fujita, F. Shimizu, *Mater. Sci. Eng. B* **96**, 159 (2002)
- 2 K. Tanaka, *Thin Solid Films* **341**, 120 (1999)
- 3 F. Rosei, *ts J. Phys.: Condens. Matter* **16**, S1373 (2004)
- 4 D. Fariás, K.-H. Rieder, *Rep. Prog. Phys.* **61**, 1575 (1998)
- 5 See, for instance, A.P. Jardine, S. Dworski, P. Fouquet, G. Alexandrowicz, D.J. Riley, G.Y.H. Lee, J. Ellis, W. Allison, *Science* **304**, 1790 (2004). Despite its high resolution in determining the scattering spectra of He atoms on a LiF surface, the assignment of the bound levels is sensitively poor compared to the optical technique proposed here
- 6 P. Treutlein et al., *Phys. Rev. Lett.* **92**, 203005 (2004)
- 7 J.M. McGuirk, D.M. Harber, J.M. Obrecht, E.A. Cornell, *Phys. Rev. A* **69**, 062905 (2004)
- 8 P. Desbiolles, J. Dalibard, *Opt. Commun.* **132**, 540 (1996)
- 9 E.A. Hinds, M.G. Boshier, I.G. Hughes, *Phys. Rev. Lett.* **80**, 645 (1998)
- 10 E.G. Lima et al., *Phys. Rev. A* **62**, 013410 (2000)
- 11 T. Passerat de Silans, B. Fariás, M. Oriá, M. Chevrollier, in *XIX International Conference on Atomic Physics (ICAP)*, 2004, p. 188
- 12 Perturbation theory for the higher-order terms of the surface potential (1) gives relative corrections of the order of  $10^{-2}$  for the adsorption energies. Then, such a refinement is worthless if one considers the actual lack of experimental data or precise calculations for this atom–surface interaction
- 13 N.W. Ashcroft, N.D. Mermin, *Solid State Physics* (Saunders College, Philadelphia, 1976), p. 368
- 14 Various potential shapes have been considered to describe the surface potential for neutral atoms, such as, for example, 12-3, 9-3, Morse; see for instance Ref. [19]
- 15 H.J. Metcalf, P. van der Straten, *Laser Cooling and Trapping* (Springer, New York, 1999)
- 16 M.A. Bouchiat et al., *Appl. Phys. B* **68**, 1109 (1999)
- 17 Z.-C. Yan, A. Dalgarno, J.F. Babb, *Phys. Rev. A* **55**, 2882 (1997)
- 18 M. Stephens, R. Rhodes, C. Wieman, *J. Appl. Phys.* **76**, 3479 (1994)
- 19 H. Hoinkes, *Rev. Mod. Phys.* **52**, 933 (1980)
- 20 E. Clementi, D.L. Raimondi, W.P. Reinhardt, *J. Chem. Phys.* **47**, 1300 (1967)
- 21 S. Magnier, M. Aubert-Frécon, *J. Quantum Spectrosc. Radiat. Transfer* **75**, 121 (2002)
- 22 M. Chevrollier et al., *Opt. Commun.* **136**, 22 (1997)
- 23 M. Mackie, J. Javanainen, *Phys. Rev. A* **60**, 3174 (1999)
- 24 The Morse potential used in our calculations reproduces these behaviors because it was adjusted to the physical potential (see Sect. 2)
- 25 A. Vardi, D. Abrashkevich, E. Frishman, M. Shapiro, *J. Chem. Phys.* **107**, 6166 (1997)
- 26 T. Passerat de Silans, M. Oriá, M. Chevrollier, to be published
- 27 O. van Kessel et al., *Nucl. Instrum. Methods Phys. Res. B* **64**, 593 (1992)
- 28 C. Henkel, S. Pötting, M. Wilkens, *Appl. Phys. B* **69**, 379 (1999)
- 29 In Ref. [7], ultra-cold atoms from a Bose–Einstein condensate probe surface-based electric fields, but the authors used a glass surface as the only dielectric material. See also Y.-J. Lin, I. Teper, C. Chin, V. Vuletic, *Phys. Rev. Lett.* **92**, 050404 (2004)
- 30 Z.W. Gortel, H.J. Kreuzer, R. Teshima, *Phys. Rev. B* **22**, 5655 (1980)
- 31 M.C. Vargas, W.L. Mochán, *Surf. Sci.* **409**, 130 (1998)
- 32 K.G.H. Vollbrecht, E. Solano, J.I. Cirac, *Phys. Rev. Lett.* **93**, 220502 (2004)